Heterotopic expression of *MPF2* is the key to the evolution of the Chinese lantern of *Physalis*, a morphological novelty in Solanaceae

Chaoying He and Heinz Saedler*

Department of Molecular Plant Genetics, Max Planck Institute for Plant Breeding Research, Carl-von-Linné-Weg 10, D-50829 Cologne, Germany

Communicated by Klaus Hahlbrock, Max Planck Institute for Plant Breeding Research, Cologne, Germany, March 8, 2005 (received for review November 28, 2004)

Morphological novelties arise through changes in development, but the underlying causes of such changes are largely unknown. In the genus *Physalis*, sepals resume growth after pollination to encapsulate the mature fruit, forming the "Chinese lantern," a trait also termed inflated-calyx syndrome (ICS). *STMADS16*, which encodes a MADS-box transcription factor, is expressed only in vegetative tissues in *Solanum tuberosum*. Its ortholog in *Physalis pubescens*, *MPF2*, is expressed in floral tissues. Knockdown of MPF2 function in *Physalis* by RNA interference (RNAi) reveals that MPF2 function is essential for the development of the ICS. The phenotypes of transgenic *S. tuberosum* plants that overexpress *MPF2* or *STMADS16* corroborate these findings: these plants display enlarged sepals. Although heterotopic expression of *MPF2* is crucial for ICS, remarkably, fertilization is also required. Although the ICS is less prominent or absent in the knockdown transgenic plants, epidermal cells are larger, suggesting that MPF2 exerts its function by inhibiting cell elongation and promoting cell division. In addition, severely affected *Physalis* knockdown lines are male sterile. Thus, heterotopic expression of *MPF2* in floral tissues is involved in two novel traits: expression of the ICS and control of male fertility. Sequence differences between the promoter regions of the *MPF2* and *STMADS16* genes perhaps reflect exposure to different selection pressures during evolution, and correlate with the observed differences in their expression patterns. In any case, the effects of heterotopic expression of *MPF2* underline the importance of recruitment of preexisting transcription factors in the evolution of novel floral traits.

MADS-box gene | morphological novelties | inflated-calyx syndrome

The origin of morphological novelties is a long-standing problem in evolutionary biology. An understanding of this process demands the elucidation of the developmental and genetic mechanisms that produce such structures. In principle, heterochrony [phylogenetic changes in the timing and rates of ontogenetic processes (1–5)] or heterotopic expression of preexisting functions (6) offer possible explanations for their appearance. In these scenarios, changes in cis-regulatory elements of genes (7) and/or changes in transacting transcriptional regulators are usually invoked.

MADS-box transcription factors determine floral meristems and floral organ identity (8–11). These proteins act as (homo- or hetero-) dimers (12, 13) or in higher-order complexes (14, 15). According to the ABC model of flower development the A-function defines sepals, A- and B-functions together define petals, B-plus C-functions control stamen development, and the C-function alone is responsible for carpel formation (9, 10, 16, 17). Most of these functions are mediated by MADS-box proteins. Their modular action is best described in the "floral quartet" hypothesis (18). The composition of oligomers in the functional complex determines the nature of the organ formed. Alterations may lead to homeotic substitutions (19). Thus, variability within such a complex could also provide a basis for the evolution of morphological novelties. For example, ectopic expression of B-function genes in whorl 1 of *Nicotiana tabacum* results in a homeotic transformation of sepals into petals: the transgenic plants form two whorls of petals (20). Recently, heterotopic expression of B-function genes has been demonstrated in *Tulipa*, which feature two whorls of petals, their characteristic tepals (6).

Morphological alterations of whorl 1 seem to be characteristic of several genera in the Solanaceae. Although most genera possess small sepals, some have extended tubular calyces. Examples include *Brugsmansia*, *Datura*, and *Nicotiana*, to name just a few. Other genera, like *Nicandra*, *Physalis* and *Withania*, display more spectacular changes, featuring a balloon-like calyx that encapsulates the mature fruit. In *Physalis*, this structure is often referred to as a "Chinese lantern," but it has also been more formally termed "inflated-calyx syndrome" (ICS) (21). In this article, we show that recruitment of an existing transcription factor to a novel context by means of heterotopic expression is apparently responsible for this novel morphological trait.

EVOLUTION

Materials and Methods

Plant Materials. The diploid and interspecific hybrid *Solanum tuberosum* × *Solanum spegazzinii* (P40) (22) and the diploid and self-compatible *Physalis pubesecens* (*syn*. *P. floridana* P106) (GenBank, Max Planck Institute for Plant Breeding Research) were grown in the greenhouse. The tetraploid *S. tuberosum* cv. Désirée (22), *Solanum macrocarpon* (PI 441915) (23) and the tetraploid *Physalis peruviana* (P105) (GenBank, Max Planck Institute for Plant Breeding Research) were also used in specific cases.

Isolation of Nucleic Acids and Expression Analysis. Total RNA was isolated by using the total RNA reagent kit (Biomol, Hamburg, Germany). DNA and RNA gel blots, preparation of probes, hybridization, and signal quantification were performed as described by He *et al*. (24). The filters were exposed to a Storage Phosphor Screen (Molecular Dynamics), and signals were quantified with a Typhoon 8600 PhosphorImager (Amersham Pharmacia).

For RT-PCR analysis, total RNA was treated with DNase I (Roche Diagnostics) to remove genomic DNA contamination. For first-strand cDNA synthesis, 4 μg of total RNA was used with reverse transcriptase (Stratagene) in a 20-μl reaction volume. For PCR of *MPF1*, the sense primer was 5′-GAG AAG CAC AAG ATG CAT TCA GAA AG-3′, and the antisense primer was 5′-GTA CCT ATA GTT AGC TAT GAC ATC ACT CTC C-3′. The flanking primers used to amplify *MPF2* were 5′-GTG CTG AGC TGA TGG AAG AAA AC-3′ and 5′-GAG AAC GAT CGA GTT CAC ATG AAC TCA TGA G-3′. The *Actin*-specific primers,

Abbreviations: ICS, inflated-calyx syndrome; RNAi, RNA interference; SEM, scanning electronic microscopy.

Data deposition: The sequences reported in this paper have been deposited in the GenBank database [accession nos. AY643725–AY643734 (cDNA sequence data), AY643735 (*MPF2*), and AY643736 (*STMADS16*)].

*To whom correspondence should be addressed. E-mail: saedler@mpiz-koeln.mpg.de.

5′-ATG GCA GAC GGA GAG GAT ATT CAG-3′ and 5′-GCA CTT CCT GTG GAC AAT AGA AGG-3′, were designed on the basis of the *S. tuberosum* actin gene sequence (X55751). The three gene-specific primer pairs were used together in the same reaction to monitor the expression of all three target genes simultaneously. PCR (annealing temperature 60°C, extension at 72°C) was performed in 50-μl volumes by using the *Taq* polymerase (Roche), and the PCR products were separated by electrophoresis on a 1.5% agarose gel.

Isolation of Genes and cDNAs, and Promoter Definition. The Expand High-Fidelity PCR System (Roche) was used for all procedures. cDNAs for *STMADS11*, *STMADS16*, and their orthologs were isolated by RACE (rapid amplification of cDNA ends) by using the 5′/3′ Rapid Amplification of cDNA Ends kit (Roche). In all, 210 5′/3′ cDNA clones were isolated from *Physalis* and sequenced. Only two gene products could be identified, *MPF1* and *MPF2*. Gene-specific primers were derived from these cDNAs and from *STMADS11* (25) and *STMADS16* cDNA (26) sequences. Genomic loci were obtained with the Expand Long Template PCR System (Roche), by using sequence-specific primers based on the full-length cDNA sequences. The promoter regions were isolated by rapid amplification of gDNA ends (RAGE) according to the Universal Genome Walker kit (Clontech). The final PCR products were cloned into the pGEM-T easy Vector (Promega). Putative transcription initiation sites were deduced from the sequences of the longest cDNA fragments obtained by 5′RACE. The *STMADS16*-promoter was defined by comparing different alleles from diploid and tetraploid lines of *S. tuberosum* that showed identical expression patterns. The conserved region from −470 to −1380 was compared with the *MPF2*-promoter.

Expression Constructs and Plant Transformation. Double-stranded RNA interference (RNAi)-mediated *MPF1* and *MPF2* knockdown was carried out in *P. pubescens*. RNAi constructs were assembled by introducing fragments of *MPF1* and *MPF2* cDNAs encoding I, K, and C domains [sense and antisense sequences, separated by a β-glucuronidase (GUS) intron] into the binary vector pFGC1008 as suggested in the ChromDB (www.chromdb.org/). These *MPF1* and *MPF2* cDNA fragments share 49% sequence identity. The primer sequences used to generate the *MPF1* fragment were 5′-CTA CTA GTG GCG CGC CAG TAT GAT GCA ACT GAT TG-3′ and 5′-CTG GAT CCA TTT AAA TAC GTA TGG ATC GGA GCT C-3′. For *MPF2*, the primers were 5′-CTA CTA GTG GCG CGC CAG CAT GAA GGA TAT CCT TG-3′ and 5′-CTG GAT CCA TTT AAA TGC TAG CTG AGT GGT AGC-3′. *Physalis* transformation was performed as described (27).

For overexpression studies, full-length *MPF1*, *MPF2*, and *STMADS16* cDNAs were cloned into the plant binary vector pBin19, introduced into LBA4404 strain of *Agrobacterium tumefaciens* and transformed into *S. tuberosum* cv. Désirée (28). The medium for shoot regeneration and for selection of transformed shoots for the RNAi knockout plants contained 1 μmol·liters^{-1} α-naphthaleneacetic acid (NAA), 12.5 μmol·liters^{-1} 6-benzylamino-purine (6-BAP) and 15 mg·liters^{-1} hygromycin. Overexpression lines were selected was on 50 mg·liters^{-1} kanamycin. *MPF2* overexpressing calli regenerated shoots at high frequency, but only a few shoots were obtained from *MPF2*-RNAi calli. Prolonged cultivation of transgenic calli occasionally resulted in regeneration. However, several of these transgenic plants did not show any phenotypic alterations relative to wild type. Therefore, *MPF2* might be essential for vegetative development, and complete knockout of its expression may be lethal.

The genotypes of transgenic lines reported in this study were verified by northern analysis by using *HPTII* (hygromycin phosphotransferase II) and *NPTII* (neomycin phosphotransferase II) as a probe in *P. pubescens* and *S. tuberosum*, respectively.

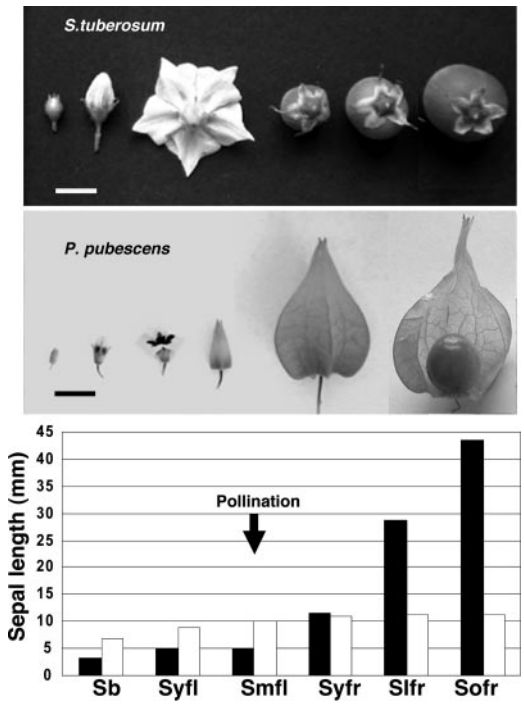

Fig. 1. Stages of flower and fruit development in *S. tuberosum* and *P. pubescens*. Sb, Syfl, Smfl, Syfr, Slfr, and Sofr are sepals from buds, young flowers, mature flowers, young fruits, large fruits, and old fruits, respectively. Open columns in the graph represent *S. tuberosum*, and filled columns represent *P. pubescens*. Pollination is indicated by an arrow. (Scale bar, 1 cm.)

Morphological Analyses and Quantification Procedures. For scanning electronic microscopy (SEM), fresh material was frozen in liquid nitrogen, sputter-coated with gold, and examined with a digital scanning microscope (DSM940, Zeiss). Five leaves and the corresponding calyces were taken from the youngest mature fruits on the main branch. Quantification of leaf areas and cell sizes was performed by using the NIH IMAGE program (IMAGEJ, available at http://rsb.info.nih.gov/nih-image). From each line, 20 mature calyces were measured.

Sequence Analysis and Phylogenetic Analysis. DNAs were sequenced at the Automatic DNA Isolation and Sequencing Unit (ADIS) of the Max Planck Institute for Plant Breeding Research (Cologne, Germany). The upstream regions of *MPF2*, *STMADS16*, and *AGL24* were scanned for potential regulatory sequences in the PLACE database [www.dna.affrc.go.jp/htdocs/PLACE database (29)]. Neighbor-joining trees were generated by PAUP 4.0 by using full-length protein sequences and SQUA from *Antirrhinum majus* (30) as the out-group.

Results

The ICS, a Morphological Novelty. Flowers of *S. tuberosum* and *P. pubescens* have small sepals that form a fused calyx basally. During flowering, the sepals of *P. pubescens* are villous, with triangular lobes, and are only ≈10% the size of the petals. In contrast to sepals of *S. tuberosum*, the calyx of *P. pubescens* resumes growth after pollination (31) to become large and five-angled at maturity, encasing the fruit (Fig. 1). This condition, the ICS (21), is not unique among the ≈96 genera of the Solanaceae (21, 32). At least 5 solanaceous genera display ICS, including all 75 species of *Physalis* (21). In all these cases, ICS is formed only after pollination.

Genes Involved in ICS Formation. Two key observations guided our search for the molecular basis of the ICS. First, the *Tunicate*

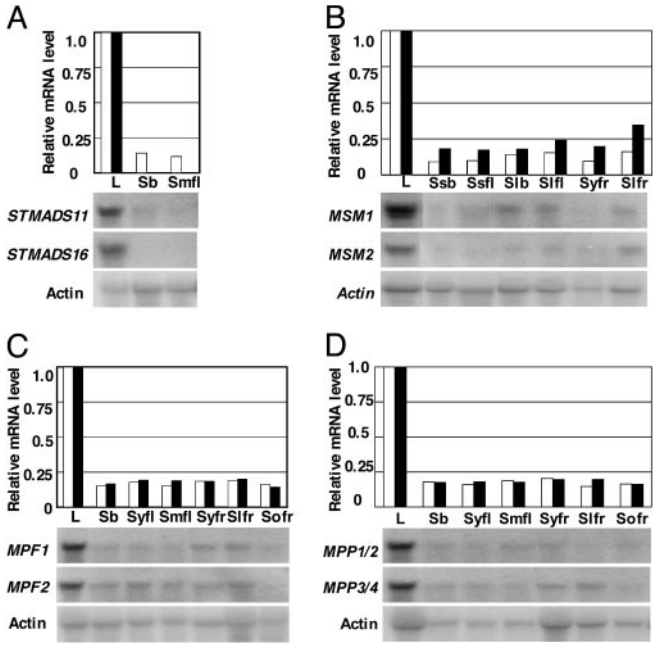

Fig. 2. Analysis of gene expression. The Northern blot studies were performed with total RNA derived from *S. tuberosum* Désirée (*A*), *S. macrocarpon* (*B*), *P. pubescens* (*C*), and *P. peruviana* (*D*). The graphs show relative mRNA levels: all values are expressed with respect to the STMADS16 (STMADS11)/Actin ratio in wild-type leaves, which was set to 1. Open bars represent *STMADS11*, and filled bars stand for *STMADS16* or their orthologs in the species as indicated. Ssb, Ssfl, Slb, and Slfl in *B* are sepals from small buds, small flowers, large buds, and large flowers, respectively, and L stands for leaves. Other abbreviations are as in the legend to Fig. 1.

phenotype in *Zea mays*, where the kernels are enclosed by glumes (21, 33, 34), apparently results from ectopic expression of the vegetative-specific MADS-box gene *ZMM19*, a *STMADS11*-like gene (35), in mutant inflorescences (21). Second, overexpression of another *STMADS11*-like gene, *STMADS16* from *S. tuberosum*, in *N. tabacum* results in the formation of leaf-like sepals (25). Therefore, a *STMADS11*-like gene, such as an ortholog of *STMADS16*, seemed likely to be involved in ICS formation in *Physalis*.

We isolated cDNAs for *STMADS11* family members from *P. pubescens*, *P. peruviana*, *S. macrocarpon*, and *S. tuberosum*. Molecular phylogeny revealed that these genes fall into the *STMADS16* and *STMADS11* subclades within the *STMADS11*-superclade (Fig. 7, which is published as supporting information on the PNAS web site). Overexpression of members of the subclades *ZMM19* (21), *SVP* (21), and *AGL24* (21, 36) in *Arabidopsis thaliana* generates enlarged, leaf-like sepals and thus suggests that they have common functions. Overexpression of *STMADS16* does not give rise to this trait in *Arabidopsis* (data not shown), but, if the gene is overexpressed in the solanaceous *N. tabacum*, foliose sepals are formed (25). This result supports the idea that a *STMADS16* ortholog might be involved in ICS formation in *Physalis*. The *Physalis* orthologs of *STMADS11* and *STMADS16* were designated *MPF1* and *MPF2*, respectively, and the gene pair *STMADS11*/*MPF1* was used as a control throughout the study. Both orthologous pairs are present as single-copy genes, as revealed by Southern analysis (refs. 25 and 26 and Fig. 8, which is published as supporting information on the PNAS web site).

Heterotopic Expression of *MPF2* Is Essential for ICS Formation. *STMADS11* and *MPF1* are expressed in leaves and in sepals of *Solanum* and *Physalis* species (Fig. 2). *STMADS16*, however, is expressed only in vegetative tissues in *S. tuberosum* (ref. 25; verified by RT-PCR in the present study; data not shown), although its ortholog *MPF2* is expressed highly in leaves and at an ≈5-fold lower level in sepals (Fig. 2 *A* and *C*) and other floral organs of *Physalis* (data not shown). Similar expression patterns for *STMADS16*-orthologous genes are also observed in *P. peruviana* and *S. macrocarpon* (Fig. 2 *B* and *D*). The observed expression patterns correlate with the presence or absence of enlarged sepals: *S. tuberosum* does not express *STMADS16* in floral tissues and displays neither ICS nor leaf-like sepals, whereas species that express orthologs of *STMADS16* in floral organs, like *P. pubescens* and *P. peruviana*, show the ICS, or have foliose sepals, like *S. macrocarpon* (ref. 21 and Fig. 2). If restriction of the *STMADS16* expression pattern to vegetative tissues represents the ancestral state, then heterotopic expression of *MPF2* in floral organs, and hence ICS formation, seems to be the derived state. We tested this hypothesis by analyzing the consequences of down-regulation of *MPF2* in transgenic *Physalis* plants using the RNAi technology, and by overexpressing *MPF2* and *STMADS16* in transgenic *S. tuberosum*.

MPF2 Function Is Required for ICS. RNA interference has been shown to be an efficient tool for gene silencing, affecting gene expression, mRNA degradation, or mRNA translation (37). In six of the eight *35S*::*MPF2*-RNAi transgenic *Physalis* plants, leaf size is reduced and formation of the "Chinese lantern" structure is impaired relative to wild type. Indeed, in the most severely affected line, Ko45, no ICS is formed (Fig. 3 *A* and *B*). Except in the case of Ko27, the reduction in the sizes of leaves and calyces correlates well with the extent to which *MPF2* RNA levels are reduced. In Ko27, the translation of *MPF2* RNA might also have been affected (Fig. 3 *A–C*). Down-regulation of *MPF2* by RNAi expression is specific, because transcripts of *MPF1*, the closest relative of *MPF2*, are not affected in the transgenic plants (Fig. 3*C*).

Interestingly, in the lines Ko34 and Ko45, in which ICS is drastically reduced or absent, a small amount of *MPF2* RNA is still detectable by multiple rounds of RT-PCR in the flowers, although Northern analysis failed to reveal gene expression (Fig. 3 *C* and *D*). This finding indicates that plant survival might depend on a residual level of *MPF2* expression (Fig. 3*D*), perhaps explaining the difficulties we encountered in obtaining transgenic knockout lines (see *Materials and Methods*).

SEM reveals that epidermal cell size in the leaves and sepals of the transgenic RNAi line Ko45 is increased by 10–30% compared with wild type (Fig. 9, which is published as supporting information on the PNAS web site), despite the overall reduction in the size of these organs (Fig. 3 *A* and *B*). This finding suggests that MPF2 negatively controls cell elongation in *Physalis* leaves and in sepals. Because cells become larger and organs smaller after down-regulation of MPF2 function, it seems that MPF2 positively controls cell proliferation in the wild type. This assumption is supported by observations made on transgenic potato plants, which overexpress *MPF2* and *STMADS16*, as shown below.

MPF2 Inhibits Cell Expansion and Promotes Cell Division. *35S*::*MPF2* or *35S*::*STMADS16* transgenic *S. tuberosum* plants form enlarged leaf-like calyces (Fig. 4*A*). SEM observations demonstrate two striking alterations in both *35S*::*MPF2* and *35S*::*STMADS16* transgenic sepals: the density of stomata is dramatically increased (Fig. 4*Bc*) as on the surface of the wild-type leaf (data not shown), and cell size is decreased by at least 50% (Fig. 4*Bc*). Given that the organ is larger and the cell size is smaller, MPF2 seems to promote cell division and to inhibit cell expansion in sepals of the transgenic potato plants. These observations support the results of our *MPF2*-RNAi analysis in *Physalis* and corroborate the key role of *MPF2* in ICS formation.

In contrast to *MPF2*, the related *Physalis* gene *MPF1*, which belongs to the *STMADS11* rather than to the *STMADS16* subclade (Fig. 7), does not affect ICS formation when inhibited using RNAi in *Physalis* (data not shown). Furthermore, when *MPF1* is overex-

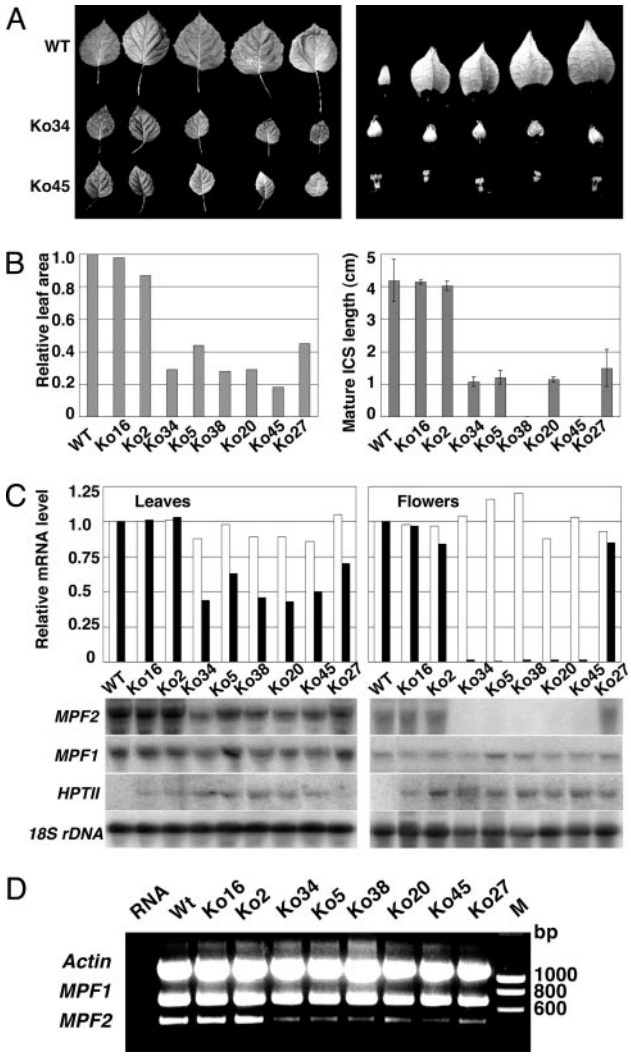

Fig. 3. MPF2 is essential for ICS formation. (*A*) Leaf size and ICS formation in the two *MPF2*-RNAi transgenic *Physalis* lines Ko34 and Ko45 compared with wild type. Shown are leaf sizes (*Left*) and calyx sizes (*Right*) during development. (*B*) Quantification of phenotypic variations among the eight *MPF2*-RNAi transgenic plants obtained. (*Left*) The relative leaf area is given; the average area of five wild-type leaves was set to 1. (*Right*) The average length of 20 mature calyces. Error bars indicate standard deviations. (*C Lower*) Northern blot analysis of RNA from leaves and flowers of wild-type and transgenic plants using the gene-specific probes indicated. (*Upper*) Expression of *MPF1* and *MPF2* in *MPF2*-RNAi plants was quantified relative to wild-type levels by using 18S rDNA for normalization. Open bars, *MPF1*; filled bars, *MPF2*. (*D*) Multiplex RT-PCR analysis of *MPF2*-RNAi plants. The expected lengths of fragments derived from the three templates *actin*, *MPF1*, and *MPF2* are 1130, 690, and 488 bp, respectively. In *MPF2*-RNAi lines, only low levels of RNA are detectable with RT-PCR. DNase I-treated total RNA was used as a negative control in the first lane. M, DNA size marker.

pressed in potato (Fig. 4*A*), calyx size, epidermal cell size, and cell number are not affected (Fig. 4*Bb*). These observations thus support the specificity of MPF2 function in ICS formation.

MPF2 Is Required for Male Fertility. Although *MPF1* RNAi transgenic *Physalis* plants are perfectly fertile, severely affected transgenic RNAi *MPF2* knockout lines, like Ko45, are almost entirely sterile. The wild-type stigma shown in Fig. 5 is loaded with pollen, and the developing berry displays good seed set (Fig. 5 *A–C*). In contrast, the transgenic line Ko45 shows very little pollen on the stigma and only occasional fertilization of ovules (Fig. 5 *E–G*). In

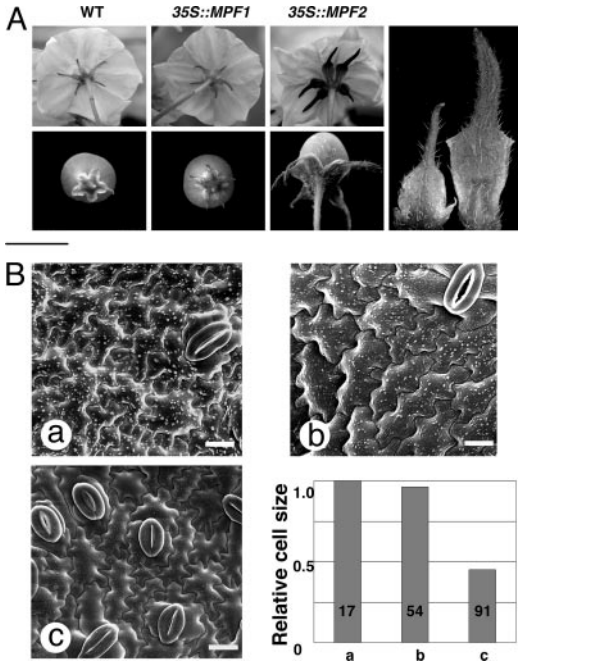

Fig. 4. Effects of overexpression of *MPF2* in transgenic lines of *S. tuberosum*. (*A*) Phenotypes of wild-type and transgenic *S. tuberosum* plants. Flowers and fruits from wild-type and transgenic plants (genotypes indicated above the panels) are shown. (*Far Right*) Sepals from wild-type (left) and *35S*::*MPF2* plants (right). (*B*) SEMs of the abaxial epidermis of mature flowers and quantification of cell size relative to the wild type. The number of cells measured is given in the columns. (*Ba*) Wild type. (*Bb*) *35S*::*MPF1* plant. (*Bc*) *35S*::*MPF2* plant. (Scale bar, 20 μm.)

F_2 plants grown from the few seeds obtained by selfing, the traits small leaves, small ICS, and reduced male fertility cosegregated with the transgene. However, upon fertilization with wild-type pollen, berries developed normally, although they remained tightly enwrapped by the calyx (Fig. 5*H*), in marked contrast to the

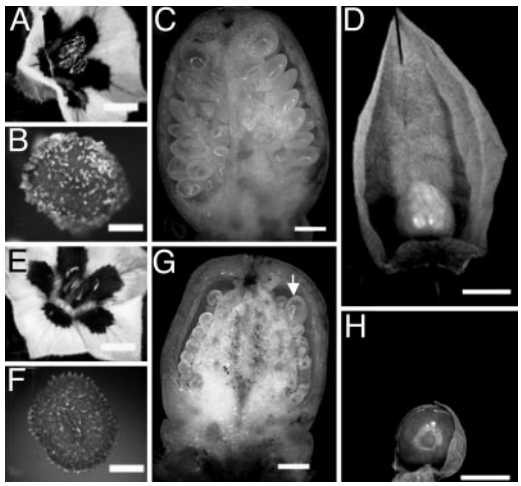

Fig. 5. MPF2 is a component of male fertility. (*A*) Wild-type flower. (*B*) Stigma covered with pollen. (*C*) Unripe berry cut open to reveal the developing seeds. (*D*) Berry inside ICS (front portion removed). (*E*) Flower from transgenic line Ko45. (*F*) No pollen on stigma. (*G*) Unripe berry cut open to reveal the unfertilized ovules. One developing seed is indicated by the arrow. (*H*) Berry on Ko45 plant fertilized with wild-type pollen. ICS (partially removed) develops tightly around the berry. [Scale bars: 6 mm (*A* and *E*), 1 mm (*B*, *C*, *F*, and G), and 1 cm (*D* and *H*).]

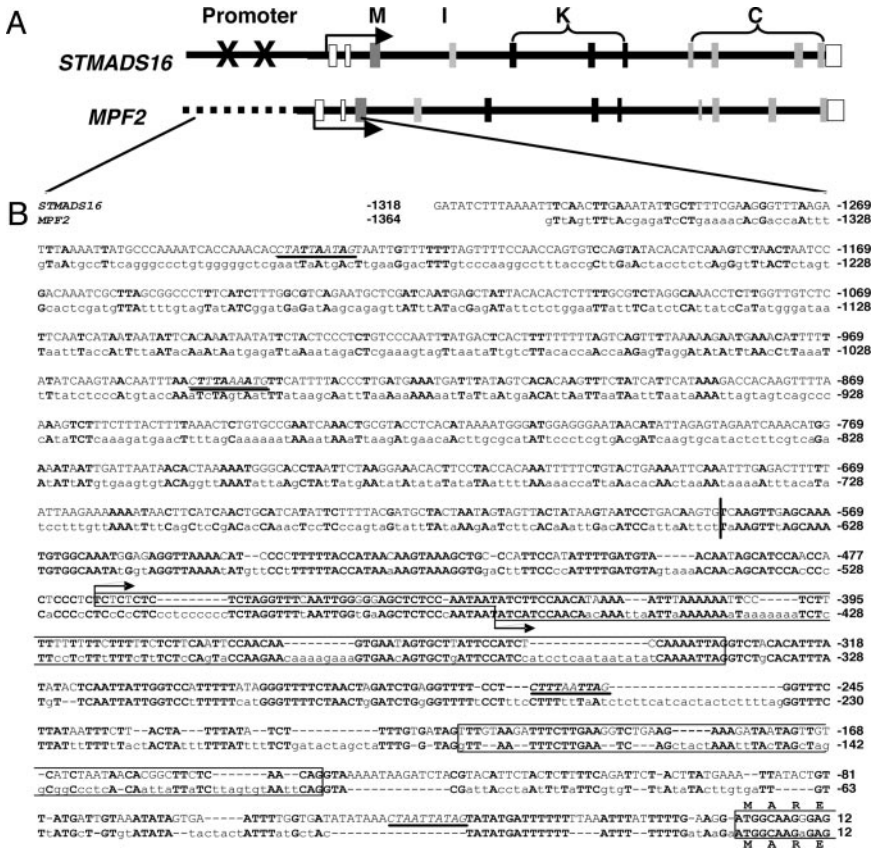

Fig. 6. Gene structures of *STMADS16* and *MPF2* (*A*) and comparison of their promoters (*B*). (*A*) The solid boxes indicate exons, and the 5′ and 3′ UTRs are depicted as open boxes. M, MADS-box (DNA-binding domain); I, intervening domain; K, keratin-like domain; C, C-terminal domain. The arrows indicate putative transcription initiation sites. Sites of sequence divergence in the promoters are highlighted by solid (*STMADS16*) or dashed lines (*MPF2*). The × symbols indicate CArG boxes in the *STMADS16*-promoter. (*B*) Bold uppercase letters indicate matching sequences, small and capital letters show divergence, and dashes reveal gaps. 5′ UTRs and part of the first translated exons are boxed. The two arrows show the putative transcription initiation sites. N10-like CArG boxes (underlined) are found only in *STMADS16*. The bold uppercase letters above the DNA sequence indicate protein sequences. The vertical line at around −560 highlights the position at which the sequences of *MPF2* (*P. pubescens*) and *MPP3* (*P. peruviana*, data not shown) deviate strongly from that of *STMADS16*.

balloon-like ICS formed in wild type *Physalis* (Fig. 5*D*). Thus, female fertility is not affected in the RNAi lines, but MPF2, in addition to its role in ICS, has apparently been integrated into the male fertility program during the evolution of *Physalis*.

Heterotopic Expression of *MPF2* Correlates with Changes in the Promoter Sequence. Recruitment of a STMADS16-like function for the establishment of the ICS in *Physalis* during evolution might have occurred in response to mutations in a transacting regulator of *MPF2* expression or to changes in cis-regulatory elements of the *MPF2* gene itself. A comparison of the molecular structure of the *STMADS16* and *MPF2* genes revealed that the organization of the transcription units, and the respective coding sequences, are highly conserved. This finding is in marked contrast to the poor conservation seen in their promoter regions (Fig. 6): although the coding sequences are 86% identical, the promoter regions show only 42% sequence identity. Intriguingly, four CArG-boxes [MADS-box protein-binding motifs (38)] are present in the *STMADS16* upstream region but absent in the corresponding part of *MPF2* (Fig. 6). This finding suggests that the promoter regions and the coding sequences of these genes have been subjected to different selective pressures during evolution. This finding is in accord with the functional similarity between the two genes in leaves as contrasted by the differences in their expression in the flowers of *S. tuberosum* and *P. pubescens*.

Unlike *STMADS16* and *MPF2*, the orthologous gene pair *STMADS11* and *MPF1* exhibit similar expression patterns (Fig. 2), suggesting that their promoters are structurally related. Indeed, both promoters contain CArG-boxes and share 60% DNA sequence identity (C.H. and H.S., unpublished data).

Thus, the sequence divergence between the *MPF2* and *STMADS16* promoters could be responsible for the heterotopic expression of *MPF2* in *Physalis*, although this assumption needs to be verified functionally.

Discussion

Gene duplication and subsequent alterations in cis-regulatory elements are often postulated to account for the evolution of new morphological features in related genera or species (7). The ICS of *Physalis* seems to be an unusual case in that it does not involve gene duplication. Here, it seems that changes in promoter structure alone were sufficient to ensure heterotopic expression of *MPF2*. *MPF2* encodes a MADS-box transcription factor that, like other MADS-box proteins in other tissues (25, 39–41), influences sepal size by controlling cell division and cell elongation.

Heterotopic *MPF2* expression is essential for ICS formation, but a signal from the developing fruit is also required for the Chinese lantern to form, because MPF2 function in controlling cell division and elongation in sepals depends on successful fertilization in *Physalis*. The precise nature of this signal is not clear; possibly, hormones can take on this role, because developing fruits produce cytokinins and gibberellins, which are known to promote either cell division or cell elongation (42–44). *MPF2* RNA is present in the sepals before pollination, and therefore the control event is likely

to be posttranslational; either the *MPF2* RNA cannot be immediately translated and the protein is synthesized only in response to the "fertilization signal," or the protein might be initially inactive and have to be activated by modification(s). Biochemical analyses of the MPF2 protein and of plant hormones before and after fertilization are required to substantiate these assumptions.

Intriguingly, in addition to controlling cell division and elongation in sepals and thus leading to ICS formation, MPF2 also plays a role in male fertility. How MPF2 became an integral part of the male fertility program during the evolution of *Physalis* and how it performs this function is not clear. Protein–protein interaction studies might reveal whether or not MPF2 replaces a component in the "floral quartets" (18). The transition from the fertility system in the progenitor, which still needs to be identified, to the fertility system of *Physalis* is the next challenge in understanding the sequence of events in the evolution of the morphological novelty termed the ICS.

Heterotopic expression of *MPF2* is thus a prerequisite for two novel functions of MPF2 in *Physalis*: calyx cell proliferation/cell expansion and male fertility. The need to maintain fertility thus provides a strong selective force for the maintenance of the ICS. Specific functions in calyx formation and male fertility may or may not prove to be separable for MPF2.

Recruitment of a transcription factor into a new context can be achieved by changes in transacting regulators or by mutations that affect cis-elements in the regulatory sequences of the transcription factor itself (5, 45). Although the *STMADS16* promoter contains two N10-like CArG-boxes, the promoter of *MPF2* in *Physalis* has no such motifs (Fig. 6). The presence or absence of CArG-boxes suggests a mechanism of regulation. Expression of MADS-box genes is often subject to autoregulation (13, 46), or is under the control of other MADS-box proteins (36), suggesting that *STMADS16* might be under the negative control of another MADS-box protein that prevents its expression in floral organs of *S. tuberosum*. SQUA-like proteins (30) are candidates for such a regulatory role, because loss of their function in, for instance, the *Arabidopsis ap1* mutant (47), or in the *lemads-mc* mutant of *Solanum lycopersicum* (tomato) (48), a close relative of potato and *Physalis*, results in enlarged and leaf-like sepals. Furthermore, *AGL24*, which codes for an STMADS16 ortholog (Fig. 7), is ectopically expressed in *Arabidopsis ap1* mutants (36). This finding is consistent with the presence of two N10-like CArG-boxes in the *AGL24* upstream region (data not shown) and supports the idea that AP1 represses its expression in floral tissues (36). SQUA homodimers have been shown to bind efficiently to N10-like CArG-boxes, whereas heterodimers of SQUA with other MADS-box proteins do not (49). SQUA-like proteins such as LeMADS-MC (48) and AP1 (47), therefore, seem to restrict the expression of *STMADS16*-like genes to vegetative tissues. *Lemads-mc* and *ap1* mutants are characterized by large, foliose sepals, possibly due to ectopic expression of the *STMADS16*-like gene (36, 48). Accordingly, the absence of N10-like CArG-boxes in the promoter of *MPF2* of *P. pubescens* seems to be a prerequisite for the expression of this gene in floral tissues.

The differential expression patterns of *STMADS16* and *MPF2* correlate with differences in calyx structure of *S. tuberosum* and *P. pubescens*. Changes in the expression of *MPF2* during evolution might have been effected by accumulating mutations in the promoter regions or by a recombination event that led to a promoter exchange. Preliminary experiments suggest that the sequences of *MPF2* (*P. pubescens*) and *MPP3* (*P. peruviana*) promoters both diverge from that of the *STMADS16* promoter of *S. tuberosum* at the same site. For this reason, we favor a recombination event that fused the coding region of an *STMADS16-like* precursor gene to a novel promoter sequence as the cause of the change in the tissue-specific expression of *MPF2*. This assumption needs to be further substantiated. Regardless of the precise reason in this particular case, recruitment of an existing transcription factor into a different functional context might be a common phenomenon in the evolution of morphological novelties (3, 50).

We thank Drs. C. Gebhardt, T. Münster, and S. Zachgo (Max Planck Institute for Plant Breeding Research) and S. Y. Chen (Genetics Institute, Chinese Academy of Sciences, Beijing) for providing plant materials and clones, and J. Hu for help in the phylogenetic reconstruction. We thank Dr. Zs. Schwarz-Sommer for comments and help in preparing the manuscript. The comments by Drs. S. Davis, T. Münster, A. Yephemov, and S. Zachgo on the manuscript are appreciated. The technical assistance of H. Henselewski and R.-D. Hirtz is gratefully acknowledged. C.H. was supported by a postdoctoral fellowship from the Max-Planck Society.

1. Raff, R. A., Parr, B. A., Parks, A. L. & Wray, G. A. (1990) in *Evolutionary Innovations*, ed. Nitecki, M. H. (Univ. of Chicago Press, Chicago), pp. 71–98.
2. Wake, D. B. & Roth, G. (1989) in *Complex Organismal Functions: Integration and Evolution in Vertebrates*, eds. Wake, D. B. & Roth, G. (Wiley, New York), pp. 361–377.
3. Keys, D. N., Lewis, D. L., Selegue, J. E., Pearson, B. J., Goodrich, L. V., Johnson, R. L., Gates, J., Scott, M. P. & Carroll, S. B. (1999) *Science* **283,** 532–534.
4. Frary, A., Nesbitt, T. C., Grandillo, S., Knaap, E., Cong, B., Liu, J. P., Meller, J., Elber, R., Alpert, K. B. & Tanksley S. D. (2000) *Science* **289,** 85–88.
5. Wang, R. L., Stec, A., Hey, J., Lukens, L. & Doebley, J. (1999) *Nature* **398,** 236–239.
6. Kanno, A., Saeki, H., Kameya, T., Saedler, H. & Theissen, G. (2003) *Plant Mol. Biol.* **52,** 831–841.
7. Doebley, J. & Lukens, L. (1998) *Plant Cell* **10,** 1075–1082.
8. Sommer, H., Beltran, J. P., Huijser, P., Pape, H., Lönnig, W. E., Saedler, H. & Schwarz-Sommer, Z. (1990) *EMBO J.* **9,** 605–613.
9. Schwarz-Sommer, Z., Huijser, P., Nacken, W., Saedler, H. & Sommer, H. (1990) *Science* **250,** 931–936.
10. Yanofsky, M., Ma, H., Bowman, J. L., Drews, G. N., Feldmann, K. A. & Meyerowitz, E. M. (1990) *Nature* **346,** 35–39.
11. Theissen, G., Becker, A., DiRosa, A., Kanno, A., Kim, J. T., Münster, T., Winter, K. U. & Saedler, H. (2000) *Plant Mol. Biol.* **42,** 115–149.
12. Davies, B., Egea-Cortines, M., de Andrade Silva, E., Saedler, H. & Sommer, H. (1996) *EMBO J.* **15,** 4330–4343.
13. Troebner, W., Ramirez, L., Motte, P., Hue, I., Huijser, P., Loennig, W. E., Saedler, H. Sommer, H. & Schwarz-Sommer, Z. (1992) *EMBO J.* **11,** 4693–4704.
14. Egea-Cortines, M., Saedler, H. & Sommer, H. (1999) *EMBO J.* **18,** 5370–5379.
15. Honma, T. & Goto, K. (2001) *Nature* **409,** 525–529.
16. Coen, E. S. & Meyerowitz, E. M. (1991) *Nature* **353,** 31–37.
17. Weigel, D. & Meyerowitz, E. M. (1994) *Cell* **78,** 203–209.
18. Theissen, G. & Saedler, H. (2001) *Nature* **409,** 469–471.
19. Theissen, G., Becker, A., Kirchner, C., Münster, T., Winter, K. U. & Saedler, H. (2002) in *Developmental Genetics and Plant Evolution*, eds. Cronk, Q. C. B., Bateman, R. M. & Hawkins, J. A. (Taylor & Francis, London), pp. 173–205.
20. Davies, B., DiRosa, A., Eneva, T., Saedler, H. & Sommer, H. (1996) *Plant J.* **10,** 663–677.
21. He, C. Y., Münster, T. & Saedler, H. (2004) *FEBS Lett.* **567,** 147–151.
22. Paal, J., Henselewski, H., Muth, J., Meksem, K., Menéndez, C. M., Salamini, F., Ballvora, A. & Gebhardt, C. (2004) *Plant J.* **38,** 285–297.
23. Furini, A. & Wunder, J. (2004) *Theor. Appl. Genet.* **108,** 197–208.
24. He, C. Y., Zhang, J. S. & Chen, S. Y. (2002) *Theor. Appl. Genet.* **104,** 1125–1131.
25. Garcia-Maroto, F., Ortega, N., Lozano, R. & Carmona, M. J. (2000) *Plant Mol. Biol.* **42,** 499–513.
26. Carmona, M. J., Ortega, N. & Garcia-Maroto, F. (1998) *Planta* **207,** 181–188.
27. Assad-Garcia, N., Ochoa-Alejo, N., Garcia-Hernandez, E., Herrera-Estrella, L. & Simpson, J. (1992) *Plant Cell Rep.* **11,** 558–562.
28. Rocha-Sosa, M., Sonnewald, U., Frommer, W., Stratmann, M., Schell, J. & Willmitzer, L. (1989) *EMBO J.* **8,** 23–29.
29. Higo, K., Ugawa, Y., Iwamoto, M. & Korenaga, T. (1999) *Nucleic Acids Res.* **27,** 297–300.
30. Huijser, P., Klein, J., Lönnig, W.-E., Meijer, H., Saedler, H. & Sommer, H. (1992) *EMBO J.* **11,** 1239–1249.
31. Martinez, M. (1998) *Anals Inst. Biol. Univ. Nac. Auton. Mex. Ser. Bot.* **69,** 71–117.
32. D'Arcy, W. G. (1991) in *Solanaceae III: Taxonomy, Chemistry, Evolution*, eds. Hawkes, J. G., Lester, R. N., Nee, M. & Estrada, N. (Royal Botanic Gardens Kew, Richmond, Surrey, U.K.), pp. 75–137.
33. Saint-Hilaire, A. (1829) *Ann. Sci. Nat.* **16,** 143–145.
34. Mangelsdorf, P. C. & Galinat, W. C. (1964) *Proc. Natl. Acad. Sci. USA* **51,** 147–150.
35. Becker, A. & Theissen, G. (2003) *Mol. Phylogenet. Evol.* **29,** 464–489.
36. Yu, H., Ito, T., Wellmer, F. & Meyerowitz, E. M. (2004) *Nat. Genet.* **36,** 157–161.
37. Baulcombe, D. (2004) *Nature* **431,** 356–363.
38. Shore, P. & Sharrocks, A. D. (1995) *Eur. J. Biochem.* **229,** 1–13.
39. Rosin, F. M., Hart, J. K., Van Onckelen, H. & Hannapel, D. J. (2003) *Plant Physiol.* **131,** 1613–1622.
40. Meyerowitz, E. M. (1997) *Cell* **88,** 299–308.
41. Davies, B., Motte, P., Keck, E., Saedler, H., Sommer, H. & Schwarz-Sommer, Z. (1999) *EMBO J.* **18,** 4023–4034.
42. Weyers, J. D. B. & Paterson, N. W. (2001) *New Phytol.* **152,** 375–407.
43. Ozga, J. A. & Reinecke, D. M. (2003) *J. Plant Growth Regul.* **22,** 73–81.
44. Kojima, K., Tamura, Y., Nakano, M., Han, D. S. & Niimi, Y. (2003) *Plant Growth Regul.* **41,** 99–104.
45. Chen, J. J., Janssen, B. J., William, A. & Sinha, N. (1997) *Plant Cell* **9,** 1289–1304.
46. Schwarz-Sommer, Z., Hue, I., Huijser, P., Flor, P. J., Hansen, R., Tetens, F., Lönnig, W.-E., Saedler, H. & Sommer, H. (1992) *EMBO J.* **11,** 251–263.
47. Mandel, M. A., Gustafson-Brown, C., Savidge, B. & Yanofsky, M. F. (1992) *Nature* **360,** 273–277.
48. Vrebalov, J., Ruezinsky, D., Padmanabhan, V., White, R., Medrano, D., Drake, R., Schuch, W. & Giovannoni, J. (2002) *Science* **296,** 343–346.
49. West, A. G., Causier, B. E., Davies, B. & Sharrocks, A. D. (1998) *Nucleic Acids Res.* **26,** 5277–5287.
50. Lee, P. N., Callaerts, P., de Couet, H. G. & Martindale, M. Q. (2003) *Nature* **424,** 1061–1065.